Catalysis Today 176 (2011) 81–87

Contents lists available at ScienceDirect

Catalysis Today

journal homepage: www.elsevier.com/locate/cattod

deNO_x over Ag/H-ZSM-5: Study of NO_2 interaction with ethanol

Rui Bartolomeu[a,b], Carlos Henriques[a], Patrick da Costa[b,1], Filipa Ribeiro[a,*]

[a] *Instituto Superior Técnico, Institute for Biotechnology and Bioengineering, Centre for Biological and Chemical Engineering, Av. Rovisco Pais, 1049-001 Lisboa, Portugal*
[b] *Université Pierre et Marie Curie, Laboratoire de Réactivité de Surface, CNRS UMR 7197, Case 178, 4 Place Jussieu, 75252 Paris Cedex 05, France*

ARTICLE INFO

Article history:
Received 8 October 2010
Received in revised form 9 February 2011
Accepted 10 February 2011
Available online 8 March 2011

Keywords:
deNO_x
Ethanol
SCR
Silver
ZSM-5 zeolite

ABSTRACT

The selective catalytic reduction of NO with ethanol in the presence of oxygen excess was studied over H-ZSM-5 and Ag/H-ZSM-5 catalysts. Temperature programmed surface reaction (TPSR) studies were performed in order to: (i) assess the effect of replacing NO by NO_2, (ii) evaluate the catalysts performance and (iii) study the formation of organic and organo-nitro compounds, as a result of nitrogen oxides and ethanol interaction.

When using NO_2 instead of NO, an almost complete conversion of NO_2 is observed on zeolite acid sites, giving rise to NO and partial oxidized hydrocarbons. NO_x conversion is higher on Ag/H-ZSM-5 (48% vs. 19%) but it is not greatly affected when NO is replaced by NO_2.

Steady-state NO_x conversion to N_2 was evaluated at 500 °C over H-ZSM-5 and Ag/H-ZSM-5 and it was found to be higher over Ag/H-ZSM-5 (48% vs. 24%). Similar NO_x conversions were attained with NO or NO_2 in reactor feed.

Formation of RNO_x compounds (CH_3NO_2), cyanides (acetonitrile) and iso-cyanates (HNCO) was shown. Ethanol reactions, such as dehydration to C_2H_4 and partial oxidation to acetaldehyde or acetic acid, were observed on the studied temperature range.

An approach to the *de*NO_x reaction mechanism over H/ZSM-5 and Ag/H-ZSM-5 catalysts was performed based on the identification by MS of several organic and organo-nitro compounds.

1. Introduction

Current and upcoming air quality regulations are requiring drastic reductions in NO_x emissions from diesel engines. Catalytic after-treatments, as SCR-HC (selective catalytic reduction with hydrocarbons), are needed in order to accomplish the necessary emission reductions. In particular, SCR with ethanol is a viable solution due to the relative environmental-friendly properties of ethanol compared to NH_3, the currently used reducer for heavy-duty vehicles [1]. Moreover, ethanol can be produced from renewable sources [2] and it can be blended with gasoline or diesel, in this last case using an emulsifier [3].

Among all catalysts tested for *de*NO_x process, Ag/Al_2O_3-based catalysts have been the subject of numerous studies [4,5], showing promising results. Silver–zeolite catalysts present similar characteristics but, in addition, they have unique ion-exchange properties.

Infrared studies have been performed to characterize the species present on the catalyst surface as well as the gas phase during *de*NO_x reaction with ethanol for Ag/Y [6] and Ag/Al_2O_3 [7–9] catalysts, in order to identify possible intermediaries and propose reaction mechanisms. Intermediate compounds such as acetaldehyde, surface acetates, enolic species, CH_3NO_2, –NCO and C_2H_4 were detected on those studies.

In this work, the catalytic reduction of NO or NO_2 with ethanol was studied, over a silver-exchanged ZSM-5 zeolite. Organic and organo-nitro compounds were continuously monitored by mass spectrometry (MS).

2. Experimental

2.1. Catalysts preparation

The parent zeolite NH_4-ZSM-5 with Si/Al = 15 was supplied by *Zeolyst International.*

The protonic form H-ZSM-5 was prepared by calcination of NH_4-ZSM-5 at a heating rate of 5 °C min^{-1} with an air flow of 4 L h^{-1} g^{-1}, kept at 200 °C for 2 h and at 500 °C for 8 h.

Ag/H-ZSM-5 catalyst was prepared by ion-exchanging twice NH_4-ZSM-5 form with a 0.01 M $AgNO_3$ (*Merck*) solution. Ion-exchange was carried out at room temperature (RT) for 24 h in the dark to avoid Ag^+ reduction. The ratio between the volume of solution and the catalyst weight (v/w) was equal to 100 mL g^{-1}.

---

[*] Corresponding author. Tel.: +351 21 841 7872; fax: +351 21 841 9198.
E-mail address: filipa.ribeiro@ist.utl.pt (F. Ribeiro).

[1] Present address: Université Pierre et Marie Curie, Paris 6, Institut Jean Le Rond d'Alembert, CNRS UMR 7190, 2 Place de la Gare de Ceinture, 78210 Saint Cyr l'école, France.

0920-5861/$ – see front matter © 2011 Elsevier B.V. All rights reserved.
doi:10.1016/j.cattod.2011.02.009

After each ion-exchange the catalyst was washed with distilled water and dried at 100 °C for 24 h. Then, the catalyst was calcined following the procedure described above.

2.2. Catalysts characterisation

Silver content in Ag/H-ZSM-5 catalyst was determined by ICP analysis and was found to be 4.4 (wt.%).

Ag species were characterized by H_2-TPR (temperature programmed reduction), diffuse reflectance UV–vis and HR-TEM (high resolution transmission electron microscopy).

H_2-TPR experiments were performed on a *Micromeritics AutoChem 2910*, using 90 mg of catalyst. Before each run, the sample was pre-treated under flowing argon (flow rate of 25 mL min^{-1}) from RT to 500 °C (10 °C min^{-1}), kept at 500 °C for 1 h and then cooled to RT. H_2-TPR was carried out under a mixture of 5% H_2/Ar with a flow rate of 30 mL min^{-1}, from RT to 950 °C at a heating rate of 10 °C min^{-1}. Hydrogen consumption was measured with a TCD (thermal conductivity detector); water was trapped in a 2-propanol/liquid nitrogen trap.

Diffuse reflectance UV–vis spectrum of the Ag/H-ZSM-5 catalyst was measured at RT with a *Varian Cary 5000 UV-Vis-NIR* spectrophotometer after heating of the sample up to 500 °C under air flow with a *Praying Mantis* accessory. H-ZSM-5 was used as reference.

HR-TEM was performed on a *JEOLJEM 2011 HR (LaB6)* microscope operating at 200 kV. Prior to HR-TEM, the sample was crushed and then dispersed without solvent addition on a carbon-coated copper TEM grid.

2.3. Catalytic tests

Catalytic tests were performed in a U-type *pyrex* reactor, under TPSR conditions. Catalysts samples (125 mg dry base) were placed over a porous plate inside the reactor and oven temperature was controlled through a *Eurotherm* temperature controller using a K-type thermocouple. In each experiment a fresh catalyst sample was used.

Before each TPSR experiment, the sample was pre-treated in flowing argon (flow rate of 250 mL min^{-1}) from RT to 500 °C (5 °C min^{-1}) and kept at 500 °C for 1 h. After catalyst reached RT, the reaction was performed with different gas mixtures: 250 ppm NO or NO_2, 750 ppm ethanol or 500 ppm propane and 0 or 7% O_2 in flowing argon. NO oxidation tests (also under TPSR conditions) were performed with a mixture of 250 ppm NO and 7% O_2. Before each TPSR, the reactant mixture was allowed to stabilize in a reactor by-pass until its composition was stable. All TPSR runs were performed with a heating rate of 10 °C min^{-1} and a total flow rate of 250 mL min^{-1}. After each TPSR, when steady-state was attained, the NO_x conversion was measured at 500 °C. The reactor outflow was continuously analysed using a combination of four different detectors. An *Eco Physics CLD 700 AL* chemiluminescence NO_x analyser allowed the simultaneous detection of NO, NO_2 and NO_x. Two *Ultramat 6* IR analysers were used to monitor N_2O, CO and CO_2. A *Pfeiffer Vacuum GSD 301* MS was used to follow the m/z signals sensible to the system perturbation: H_2O (m/z = 18), ethylene (m/z = 27 and 26), N_2/CO (m/z = 28), acetaldehyde (m/z = 29), acetonitrile (m/z = 41), –NCO (m/z = 42), acetic acid (m/z = 60) and CH_3NO_2 (m/z = 61).

3. Results and discussion

3.1. Catalysts characterisation

H_2-TPR profile of Ag/H-ZSM-5 shown in Fig. 1 evidences three H_2 consumption processes, with maxima at 140, 210 and 450 °C. No other peaks were detected above 600 °C. H_2-TPR of H-ZSM-5 does not present any peaks.

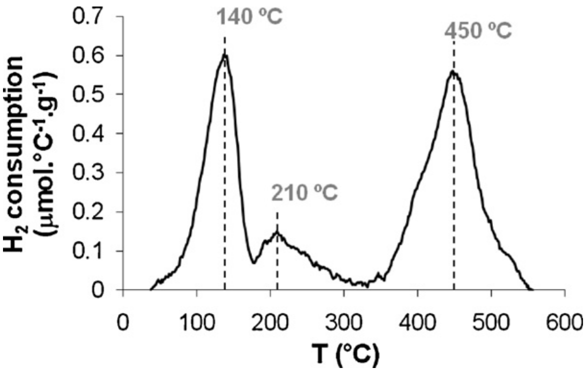

Fig. 1. H_2-TPR profile of Ag/H-ZSM-5 catalyst.

According to the literature, the first two H_2 consumption processes can be attributed to either Ag^+ on the zeolite exchange-sites [10,11] or Ag_2O [12] reduction; both species have been reported to reduce from 130 to 275 °C. The high temperature H_2 peak, with maximum at 450 °C, can be attributed to the reduction of partially charged silver clusters, $Ag_n^{\delta+}$ [11].

HR-TEM micrographs of Ag/H-ZSM-5 catalyst (Fig. 2) evidence the presence of Ag particles with a mean diameter of 2.5 ± 0.7 nm. The inter-reticular planes of the silver particles were measured (2.4 and 2.0 Å) and they were found to belong to the crystallographic planes (1 1 1) and (2 0 0), respectively, consisting on face-centered cubic metallic silver. Crystallographic planes belonging to Ag_2O were not found. The presence of Ag^0 particles on Ag/H-ZSM-5 justifies the fact that total H_2 consumption on the H_2-TPR is lower than the stoichiometric value (0.23 instead of 0.5).

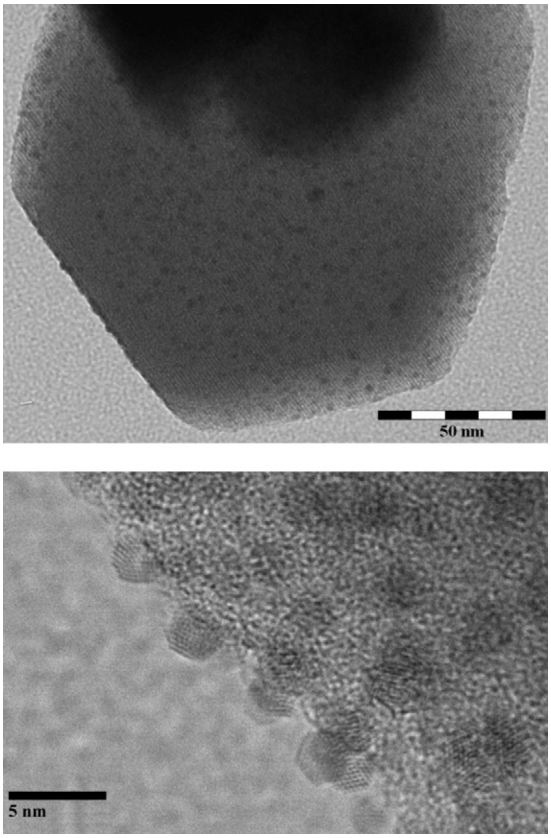

Fig. 2. HR-TEM micrographs of Ag/H-ZSM-5 zeolite crystal showing the silver particles distribution (up) and detail of a crystal with silver particles and their inter-reticular planes (down).

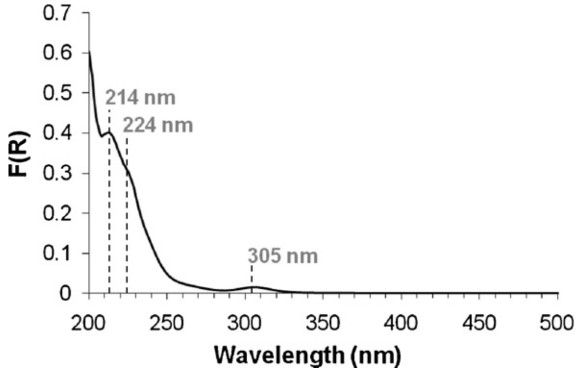

Fig. 3. Diffuse reflectance UV–vis spectrum of Ag/H-ZSM-5 catalyst at RT after heating the sample up to 500 °C under air flow.

Diffuse reflectance UV–vis spectrum of Ag/H-ZSM-5 (Fig. 3) presents three bands at 214, 224 and 305 nm. According do the literature, the first two bands can be attributed to Ag^+ on the zeolite exchange-sites [13,14] while the third band can be attributed to partially charged silver clusters, $Ag_n^{\delta+}$ [10].

Taking into account that UV–vis spectra of Ag/H-ZSM-5 at RT, under air flow, confirmed the presence of Ag^+, the two first TPR peaks can therefore be attributed to Ag^+ reduction.

3.2. Catalytic tests

3.2.1. NO oxidation

Fig. 4, which compares the NO oxidation profiles obtained for H-ZSM-5 and Ag/H-ZSM-5, shows that NO is adsorbed over H-ZSM-5 catalyst from RT until about 70 °C, while over Ag/H-ZSM-5 NO is adsorbed from RT to about 100 °C. Oxidation of NO to NO_2 starts at about 80 °C for both catalysts, according to the following reaction:

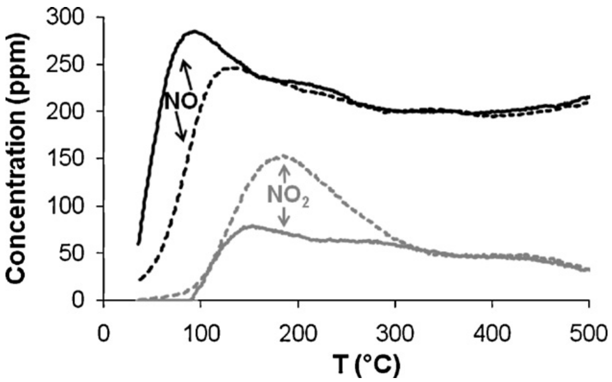

Fig. 4. NO oxidation profiles over H-ZSM-5 (▬▬▬, ▬▬▬) and Ag/H-ZMS-5 (········, ········) with 250 ppm NO and 7% O_2; total flow of 250 mL min^{-1}.

$$NO + \tfrac{1}{2}O_2 = NO_2 \qquad (1)$$

Over H-ZSM-5 catalyst, the maximum NO_2 value is 80 ppm at 150 °C and 150 ppm at 185 °C over Ag/H-ZSM-5 catalyst. NO oxidation to NO_2 takes place over the H-ZSM-5 catalyst, which means that this reaction proceeds partially over the acid sites of zeolite support. Nonetheless, the presence of Ag enhanced the catalyst ability to perform NO oxidation to NO_2 in the low temperature range (from 125 to 300 °C).

Meunier et al. [15] proposed that, over an Ag/Al_2O_3 catalyst, metallic silver enhanced the oxidation of NO to NO_2. Since metallic silver particles were observed over the Ag/H-ZSM-5 catalyst by HRTEM (as presented in Section 3.1), this observation is in line with the previous proposition of those authors.

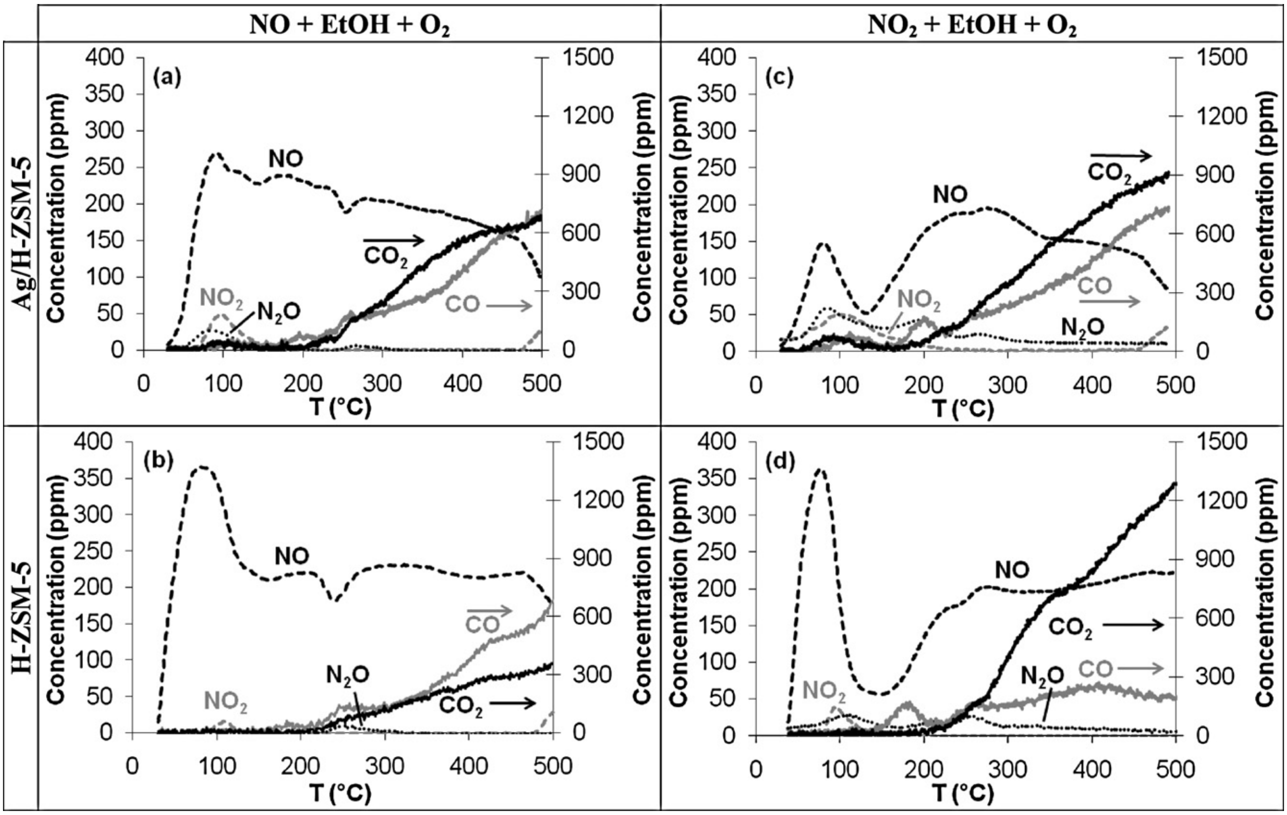

Fig. 5. TPSR profiles with 250 ppm NO, 750 ppm ethanol and 7% O_2 over (a) H-ZSM-5 and (b) Ag/H-ZMS-5 and with 250 ppm NO_2, 750 ppm ethanol and 7% O_2 over (c) H-ZSM-5 and (d) Ag/H-ZMS-5; total flow of 250 mL min^{-1}.

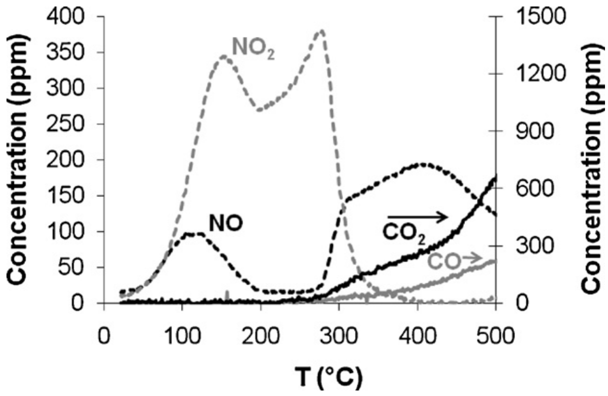

Fig. 6. TPSR profiles with 250 ppm NO$_2$, 500 ppm propane and 7% O$_2$ over Ag/H-ZMS-5; total flow of 250 mL min^{-1}.

3.2.2. NO reduction over H-ZSM-5 and Ag/H-ZSM-5

Fig. 5(a) shows TPSR of Ag/H-ZSM-5, which was performed with 750 ppm ethanol, 7% O$_2$ and 250 ppm NO. NO adsorbs on the catalyst from RT until 80 °C and reaches a small desorption maximum at 90 °C, after which NO concentration is always below 250 ppm. Over H-ZSM-5 (Fig. 5(b)), there is a NO adsorption from RT to 55 °C, followed by a greater desorption maximum at 80 °C. The greater NO desorption over H-ZSM-5 compared to Ag/H-ZSM-5 can be explained by the formation of N$_2$O and NO$_2$ presence on the Ag/H-ZSM-5 TPSR, which practically does not occur over H-ZSM-5.

A maximum NO$_x$ conversion of 48% is reached at 500 °C over Ag/H-ZSM-5 (Fig. 5(a)). A small N$_2$O formation occurs at low temperature (maximum of 25 ppm at 80 °C). On the other hand, H-ZSM-5 catalyst (Fig. 5(b)) has a small N$_2$O formation (maximum of 10 ppm at 250 °C) and a low NO$_x$ conversion (maximum of 19% at 500 °C).

Concerning ethanol conversion into CO$_x$, over H-ZSM-5 catalyst, there is similar hydrocarbon conversion to CO but lower conversion to CO$_2$ compared to Ag/H-ZSM-5.

It should be noted that repeating runs with the same sample showed that no catalyst deactivation occurred in the studied temperature range over both catalysts.

3.2.3. NO$_2$ reduction over H-ZSM-5 and Ag/H-ZSM-5

When NO is replaced by NO$_2$ in the feed, completely different NO$_x$, N$_2$O and CO$_x$ concentration profiles are obtained in the TPSR experiments performed with Ag/H-ZSM-5 (Fig. 5(c)). The most notorious feat is that almost no NO$_2$ is detected on reactor exit through the experiment. Therefore, almost all NO$_2$ fed to the reactor was converted into NO. In another TPSR run made with 500 ppm propane, 7% O$_2$ and 250 ppm NO$_2$ (Fig. 6), this almost complete NO$_2$ conversion to NO did not take place. As such, this reaction only occurs when ethanol is co-fed with NO$_2$ and it takes place even in the absence of O$_2$ (Fig. 7(a)). It should also be noted that conversion of NO$_2$ occurs at RT and immediately after the feed was put into contact with the catalyst. A gas-phase reaction between ethanol and NO$_2$ can be discarded because, in the by-pass made before the TPSR, only NO$_2$ was detected by the NO$_x$ analyser. Furthermore, this NO$_2$ conversion to NO is also verified over H-ZSM-5 (Fig. 5(d)). Therefore, ethanol must react with NO$_2$ over the zeolite acid sites to originate NO and partially oxidized hydrocarbons (such as acetaldehyde) according to the following reaction:

$$NO_2 + C_2H_5OH = NO + CH_3CHO + H_2O \quad (2)$$

Yeom et al. [6] had already observed acetaldehyde by IR spectroscopy performed over a silver-exchanged Y zeolite. However, acetaldehyde ($m/z = 29$) was not detected by MS until about 120 °C (Fig. 8), which could be explained by adsorption on the zeolite until this temperature.

Moreover, following the desorption maximum, a great decrease in NO concentration, which leads to a minimum of 50 ppm of NO at 130 °C, occurs (Fig. 5(c)). This decline in NO concentration is not accompanied by an increase in N$_2$O or N$_2$ ($m/z = 28$, not shown), meaning that NO concentration does not decrease due to conversion into N$_2$O (unselective catalytic reduction) or N$_2$ (selective catalytic reduction). However, N$_2$O formation occurs with two maxima, one at 80 °C and a second one at 200 °C.

Analysing now CO and CO$_2$ concentration profiles for the TPSRs experiments over H-ZSM-5 and Ag-H/ZSM-5 (Fig. 5), in the presence of NO$_2$ instead of NO, there is more CO$_2$ formation. It seems that NO$_2$ presence promotes total hydrocarbon oxidation which leads to CO$_2$. This feat is more pronounced over H-ZSM-5.

3.2.4. Steady-state NO$_x$ conversion to N$_2$ at 500 °C

N$_2$ formation is difficult to identify by mass spectrometry due to interference with CO ($m/z = 28$). Therefore, only when there is no CO formation it is possible to clearly attribute the fragment $m/z = 28$ to N$_2$, which is only valid in the low temperature region of the TPSR tests. Therefore, in order to evaluate N$_2$ formation, which comes from *de*NO$_x$ reaction, steady-state conversion points were taken at 500 °C. Assuming that there are no adsorbed N-containing species over the catalyst surface and that the only N-containing species exiting the reactor are NO, NO$_2$, N$_2$O and N$_2$, a mass balance to N-containing species can be made in order to obtain the amount of formed N$_2$ at 500 °C. The results of this mass balance are presented in Table 1. It can be seen that the higher N$_2$ yield (48%) is obtained over Ag/H-ZSM-5 when NO$_2$ is used instead of NO in the reactor feed. It seems that NO$_2$ presence enhances N$_2$ formation over Ag/H-ZSM-5. On the other hand, H-ZSM-5 catalyst shows significantly

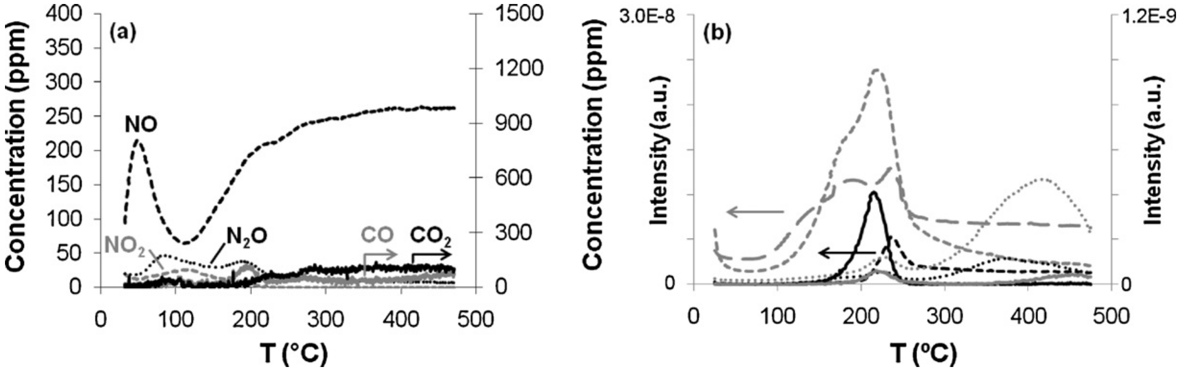

Fig. 7. TPSR (a) and MS (b) profiles of H$_2$O (— —), ethylene (- - -), acetaldehyde (- - -), acetonitrile (………), –NCO (………), acetic acid (——) and CH$_3$NO$_2$ (——) with 250 ppm NO$_2$ and 750 ppm ethanol over Ag/H-ZMS-5; total flow of 250 mL min^{-1}. Acetic acid and CH$_3$NO$_2$ signals were multiplied by 50.

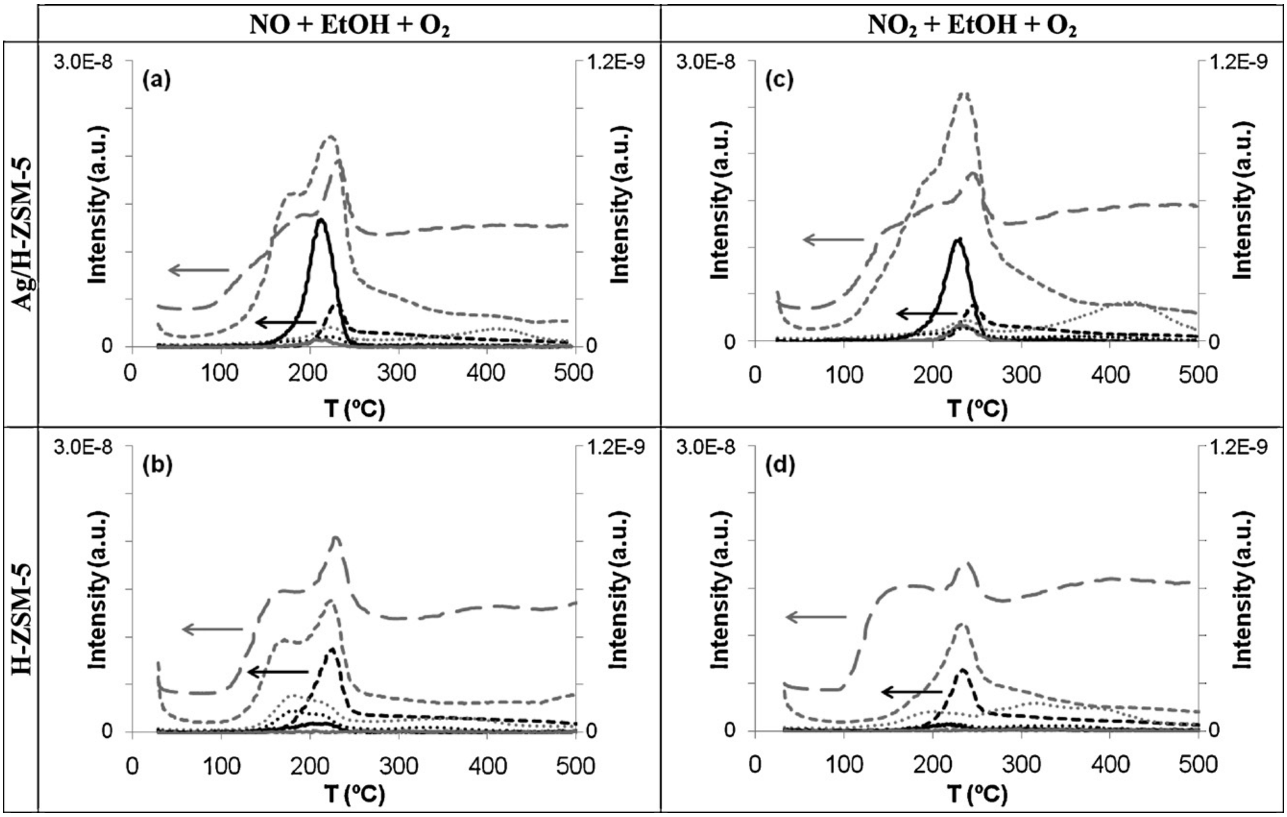

Fig. 8. MS profiles of H_2O (▬ ▬), ethylene (▬ ▬ ▬), acetaldehyde (– – –), acetonitrile (··········), –NCO (·········), acetic acid (▬▬▬) and CH_3NO_2 (▬▬▬) with 250 ppm NO, 750 ppm ethanol and 7% O_2 over (a) H-ZSM-5 and (b) Ag/H-ZMS-5 and with 250 ppm NO_2, 750 ppm ethanol and 7% O_2 over (c) H-ZSM-5 and (d) Ag/H-ZMS-5; total flow of 250 mL min^{-1}. Acetic acid and CH_3NO_2 signals were multiplied by 50.

lower N_2 yields (21 and 24%). Moreover, NO replacement by NO_2 in the reactor feeds does not affect N_2 yield.

3.2.5. MS analysis of reactor outlet

For all performed TPSR experiments, ethylene (m/z = 27 and 26) and H_2O (m/z = 18) formation maxima were detected by MS at around 240 °C, as can be seen in Figs. 7(b) and 8. It is well known that zeolites are effective catalysts for ethanol dehydration to ethylene, due to their acidity:

$$C_2H_5OH = C_2H_4 + H_2O \qquad (3)$$

Moreover, it was reported [16,17] that this reaction proceeds over H-ZSM-5 type catalyst on the temperature range of 200–300 °C, which is consistent with the temperature at which the ethylene and H_2O peaks were detected. It should be noticed that, at the same temperature of ethylene and water peaks, NO consumption can also be found in all TPSR runs. Taking into account that N_2 (m/z = 28, not shown) formation was also detected in the TPSR performed with 250 ppm NO_2 and 7% O_2 (Fig. 7), this minimum can therefore be correlated with C_2H_4 formation, which could act as a NO reducing agent.

Over Ag/H-ZSM-5 catalyst, reaction (3) is still present, but at smaller scale: C_2H_4 peak in Ag/H-ZMS-5 is smaller than in H-ZSM-5. This could be explained by a lower amount of ethanol available to take part in this reaction due to other reaction pathways catalysed by Ag leading to ethanol consumption. One of these reactions can be the ethanol oxidation by O_2 or NO_2 to acetic acid (m/z = 60), which can be described by the following global process [6]:

$$C_2H_5OH + O_2\,(\text{or}\,2NO_2) = CH_3COOH + H_2O\,(+2NO) \qquad (4)$$

In fact, an acetic acid peak with a maximum between 210 and 230 °C was detected on the TPSR experiments performed with Ag/H-ZSM-5 (Fig. 8a and c), but only a small amount was detected with H-ZSM-5 (Fig. 8(b) and (d)). In the absence of O_2, (Fig. 7(b)), this reaction still occurs, which is an evidence of NO_2 participation in reaction (4). This process can be decomposed in two steps [6]:

$$NO_2 + C_2H_5OH = NO + CH_3CHO + H_2O \qquad (2)$$

$$NO_2 + CH_3CHO = NO + CH_3COOH \qquad (5)$$

Acetaldehyde (m/z = 29) is detected on TPSRs performed with H-ZSM-5 or Ag/H-ZSM-5 and acetic acid (m/z = 60) is only detected

Table 1
NO, NO_2 and N_2O concentrations analysed during reaction performed under steady-state conditions at 500 °C with 250 ppm NO or NO_2, 750 ppm ethanol and 7% O_2. N_2 concentrations were calculated by mass balance to N-containing species.

		NO (ppm)	NO_2 (ppm)	N_2O (ppm)	N_2 (ppm)	N_2 yield (%)[a]
Ag/H-ZSM-5	NO + EtOH + O_2	162	0	0	44	35
	NO_2 + EtOH + O_2	129	0	0	60	48
H-ZSM-5	NO + EtOH + O_2	122	67	0	30	24
	NO_2 + EtOH + O_2	182	16	0	26	21

[a] N_2 yield = 2 × N_2 formed/NO_x in reactor feed

on the second case, suggesting that reaction (5) is metal-catalysed, taking place over Ag.

The same is valid for CH_3NO_2 (m/z = 61), which is detected around 215 °C only over the Ag/H-ZSM-5 catalyst (Figs. 7(b), 8(a) and (c)). This compound can be assumed as an RNO_x-type molecule, which results from the interaction between acetic acid and NO_2 [6], and according to several authors, it is a possible intermediary in *de*NO_x process [18,19].

On the other hand, the –NCO fragment (m/z = 42), probably coming from HNCO molecule, another possible intermediary in *de*NO_x chemistry [18], was also detected above 300 °C in the presence of either NO or NO_2 over both catalysts, H-ZSM-5 and Ag/H-ZSM-5. It should be noticed that the m/z = 42 fragment can also come from acetaldehyde fragmentation. However, analysis of m/z = 29, the main fragment of acetaldehyde molecule, shows that this fragment does not follow the same trend of m/z = 42 fragment above 300 °C. This means that, above this temperature, m/z = 42 fragment does not come from acetaldehyde, but instead from the –NCO fragment.

When only 750 ppm ethanol and 250 ppm NO_2 are used to perform the TPSR (Fig. 7(b)), the peak of the –NCO fragment (m/z = 42) becomes more intense. CH_3NO_2 (m/z = 61) formation was also detected from 400 °C up to 500 °C. It is clear that, in O_2 absence, there is no combustion of these compounds to CO_x and H_2O. Furthermore, after a TPSR with 750 ppm ethanol and 250 ppm NO_2, the Ag/H-ZSM-5 catalyst becomes much darker than after a TPSR with 750 ppm ethanol, 7% O_2 and 250 ppm NO_2, evidencing that hydrocarbon species or coke deposition over the catalyst is higher in O_2 absence.

Another organo-nitro compound that was detected by MS is acetonitrile (m/z = 41). This compound started to form at around 150 °C in all TPSR experiments. With 750 ppm ethanol and 250 ppm NO_2 (Fig. 7(b)), a large acetonitrile peak appeared from 300 °C to 500 °C.

The possibility of gas-phase reactions was not evaluated. According to Niki et al. [20], NO_2 can react with ethanol according to the following reaction:

$$C_2H_5OH + NO_2 = C_2H_5ONO + HNO_3 \qquad (6)$$

However, detection of C_2H_5ONO (ethyl nitrite) by MS is rather difficult because its three main mass fragments are common to NO (m/z = 30), acetaldehyde (m/z = 29) and acetic acid (m/z = 60). Thus, the possibility of ethyl nitrite formation on the gas-phase or over the catalyst could not be evaluated with the available experimental apparatus.

3.2.6. *de*NO_x mechanism approach

The detection by MS of several organic and organo-nitro compounds allows to have an insight on the *de*NO_x reaction mechanism over H/ZSM-5 and Ag/H-ZSM-5 catalysts. Moreover, information about the active sites (acid sites or metallic sites) can be obtained.

According to the mechanism proposed by several authors [21,22], the first step in SCR-HC with NO is oxidation of NO to NO_2 (reaction (1)). This reaction can take place over the zeolite acid sites, but metallic sites can also participate and have a higher ability to perform the oxidation of NO to NO_2, as it was shown previously in Section 3.2.1. Moreover, this reaction is not the rate-limiting step on the NO_x conversion to N_2 because similar NO_x conversions are attained when NO is replaced by NO_2 in the reactor feed.

The second step is the oxidation of the reducer (HC) by the NO_2, producing partial oxidized hydrocarbon species (HC_xO_y) and NO:

$$NO_2 + HC = HC_xO_y + NO \qquad (7)$$

This function corresponds to reactions (2) and (5), with either acetaldehyde or acetic acid as the partial oxidized hydrocarbon species. This function takes place over the zeolite acid sites but is greatly enhanced when silver is added to the zeolite, leading to a higher formation of acetaldehyde and acetic acid (Fig. 8). Taking into account that all NO_2 is transformed into NO when the TPSR runs are performed with NO_2 in the feed, it is clear that this function is highly effective over H-ZSM-5 and Ag/H-ZSM-5 catalysts.

Finally, the third function of the mechanism involves the reduction of NO to N_2 and the oxidation of the HC_xO_y species:

$$HC_xO_y + 2NO = N_2 + H_2O + CO_2 \qquad (8)$$

This step seems to be favoured over the metallic sites, because higher NO_x conversions are attained over Ag/H-ZSM-5. CH_3NO_2 and HNCO species identified by MS (Figs. 7(b) and (8)) correspond to intermediate species of the third function. As NO_x conversion was not observed during the TPSR performed with 750 ppm ethanol and 250 ppm NO_2 over Ag/H-ZSM-5 (Fig. 7), it becomes clear that O_2 must be needed in some intermediary step of reaction (8) to transform HNCO and CH_3NO_2. This is corroborated by a higher amount of these species detected by MS during this TPSR.

4. Conclusions

A combination of characterisation techniques (H_2-TPR, HR-TEM and UV–vis spectroscopy) allowed the identification of Ag^+ and Ag^0 species over Ag/H-ZSM-5. TPSR experiments with NO and O_2 over this catalyst showed that it possesses the ability to oxidize NO to NO_2. A maximum of 150 ppm NO_2 is attained at 185 °C.

When NO is replaced by NO_2, NO_x conversion is not significantly affected on the high temperature range (above 300 °C) over H-ZSM-5 and Ag/H-ZSM-5 catalysts. On the other hand, a reaction between ethanol and NO_2 over these catalysts converts all NO_2 to NO, while forming partial oxidized hydrocarbons such as acetaldehyde.

Ethanol reactions, such as dehydration to C_2H_4 and partial oxidation to acetaldehyde or acetic acid, were also observed on the studied temperature range.

Steady-state NO_x conversion to N_2 was evaluated at 500 °C over H-ZSM-5 and Ag/H-ZSM-5 and it was found to be higher over Ag/H-ZSM-5 (48% vs. 24%). Similar NO_x conversions were attained with NO or NO_2 in reactor feed.

Formation of RNO_x compounds (CH_3NO_2), cyanides (acetonitrile) and iso-cyanates (HNCO) was put into evidence. These compounds can be intermediaries of the *de*NO_x process. Nonetheless, *de*NO_x activity with ethanol is rather low under the tested conditions: maximum NO_x conversion of 48% is obtained at 500 °C over Ag/H-ZSM-5 catalyst.

Detection by MS of several organic and organo-nitro compounds allowed an approach to the *de*NO_x reaction mechanism over H/ZSM-5 and Ag/H-ZSM-5 catalysts.

Acknowledgements

The authors wish to thank to Fundação para a Ciência e Tecnologia (FCT) for financial support (grant number SFRH/BD/44108/2008 and project number PTDC/EQU-ERQ/102771/2008) and Sandra Casale for performing HR-TEM.

References

[1] S. Roy, M.S. Hegde, G. Madras, Applied Energy 86 (2009) 2283.
[2] G.W. Huber, S. Iborra, A. Corma, Chem Rev 106 (2006) 4044.
[3] X. Shi, Y. Yu, H. He, S. Shuai, H. Dong, R. Li, Journal of Environmental Sciences 20 (2008) 177.
[4] K. Arve, L. Capek, F. Klingstedt, K. Eranen, L.E. Lindfors, D.Y. Murzin, J. Dedecek, Z. Sobalik, B. Wichterlova, Top Catal 30-1 (2004) 91.
[5] A. Musi, P. Massiani, D. Brouri, J.-M. Trichard, P. Da Costa, Catal Lett 128 (2009) 25.
[6] Y.H. Yeom, M.J. Li, W.M.H. Sachtler, E. Weitz, J Catal 246 (2007) 413.
[7] Y.H. Yeom, M. Li, W.M.H. Sachtler, E. Weitz, J Catal 238 (2006) 100.

[8] Y. Yu, H. He, Q. Feng, H. Gao, X. Yang, Appl Catal B: Environ 49 (2004) 159.
[9] T. Chafik, S. Kameoka, Y. Ukisu, T. Miyadera, J Mol Catal A: Chem 136 (1998) 203.
[10] J. Shibata, K.-i. Shimizu, Y. Takada, A. Shichi, H. Yoshida, S. Satokawa, A. Satsuma, T. Hattori, J Catal 227 (2004) 367.
[11] A. Ausavasukhi, S. Suwannaran, J. Limtrakul, T. Sooknoi, Applied Catalysis A: General 345 (2008) 89.
[12] K.A. Bethke, H.H. Kung, J Catal 172 (1997) 93.
[13] P. Sazama, H. Jirglová, J. Dedecek, Mater Lett 62 (2008) 4239.
[14] C. Shi, M. Cheng, Z. Qu, X. Bao, Appl Catal B: Environ 51 (2004) 171.
[15] F.C. Meunier, J.P. Breen, V. Zuzaniuk, M. Olsson, J.R.H. Ross, J Catal 187 (1999) 493.
[16] C. de las Pozas, R. Lopez-Cordero, J.A. Gonzalez-Morales, N. Travieso, R. Roque-Malherbe, J Mol Catal 83 (1993) 145.
[17] X. Zhang, R. Wang, X. Yang, F. Zhang, Microporous Mesoporous Mater 116 (2008) 210.
[18] K.-i. Shimizu, K. Sugino, K. Kato, S. Yokota, K. Okumura, A. Satsuma, The Journal of Physical Chemistry C 111 (2007) 6481.
[19] Y. Yeom, M. Li, A. Savara, W. Sachtler, E. Weitz, Catal Today 136 (2008) 55.
[20] H. Niki, P.D. Maker, C.M. Savage, L.P. Breitenbach, Int J Chem Kinet 14 (1982) 1199.
[21] G. Djéga-Mariadassou, Catal Today 90 (2004) 27.
[22] O. Gorce, F. Baudin, C. Thomas, P. Da Costa, G. Djéga-Mariadassou, Appl Catal B: Environ 54 (2004) 69.